

RESEARCH PAPER



Phosphonate inhibitors of West Nile virus NS2B/NS3 protease

Marcin Skoreński^a, Aleksandra Milewska^{b,c}, Krzysztof Pyrc^{b,c}, Marcin Sieńczyk^a and Józef Oleksyszyn^a

^aFaculty of Chemistry, Division of Medicinal Chemistry and Microbiology, Wrocław University of Science and Technology, Wrocław, Poland;

^bFaculty of Biochemistry, Biophysics and Biotechnology, Microbiology Department, Jagiellonian University, Krakow, Poland; ^cLaboratory of Virology, Malopolska Centre of Biotechnology, Jagiellonian University, Krakow, Poland

ABSTRACT

West Nile virus (WNV) is a member of the flavivirus genus belonging to the *Flaviviridae* family. The viral serine protease NS2B/NS3 has been considered an attractive target for the development of anti-WNV agents. Although several NS2B/NS3 protease inhibitors have been described so far, most of them are reversible inhibitors. Herein, we present a series of α -aminoalkylphosphonate diphenyl esters and their peptidyl derivatives as potent inhibitors of the NS2B/NS3 protease. The most potent inhibitor identified was Cbz-Lys-Arg-(4-GuPhe)^P(OPh)₂ displaying K_i and k_2/K_i values of 0.4 μ M and 28 265 M⁻¹s⁻¹, respectively, with no significant inhibition of trypsin, cathepsin G, and HAT protease.

ARTICLE HISTORY

Received 22 September 2017

Revised 17 July 2018

Accepted 25 July 2018

KEYWORDS

NS2B/NS3 protease; aminophosphonates; serine proteases; enzyme inhibitors; West Nile virus

Introduction



The West Nile virus (WNV) belongs to the *flavivirus* genus (*Flaviviridae* family) and is a mosquito-borne human pathogen of global occurrence. WNV was first isolated from humans in 1937 in the West Nile district of Uganda¹. In 1953, it was identified in birds of the Nile delta region. Until 1997, WNV was not considered pathogenic to birds when a more virulent strain appeared in Israel and caused fatal disease with signs of encephalitis and paralysis in various bird species. In 1999, a pathogenic WNV strain was transferred to New York leading to its rapid spread throughout the USA, Canada and in the following years, the virus further spread, reaching northern countries of South America². The virus also became a relevant human pathogen in Eurasia, causing large outbreaks in Greece, Israel, Romania, and Russia^{3–6}. Although the life-cycle of WNV involves the transmission of viruses between birds and mosquitoes, various mammalian species, including humans, and horses, are susceptible to the virus. However, mammals are generally dead-end hosts, being infected through the bites of infected mosquitoes⁷. Although infections with WNV are mainly asymptomatic, one-fifth of the infected humans develops symptoms of the milder West Nile fever or more severe neuroinvasive diseases (meningitis and encephalitis). Unfortunately, no vaccine or effective antiviral therapy against WNV is available⁸.


The flaviviral genome is a positive-sense single strand RNA. The viral replication process occurs in the cytoplasm where the RNA serves as a template for production of a large polyprotein, which is further processed by host and viral proteases. This proteolytic maturation yields structural (C, prM, and E) and non-structural proteins (NS1, NS2A, NS2B, NS3, NS4A, NS4B, and NS5). NS3 plays a key role during the polyprotein processing. This protein is composed of an N-terminal protease domain (1–179 amino acids) and a C-terminal helicase domain (residues 180–618). It has been

demonstrated that inactivation of NS2B/NS3 protease catalytic centre blocks viral replication⁸. To become fully functional, the NS3 segment requires a short co-factor, NS2B. The WNV protease contains the classical serine protease catalytic triad Asp-His-Ser. The protease binding site exists as a shallow groove composed of 7 subsites (S4–S3', according to the Schechter and Berger nomenclature)⁹. An analysis of the substrate preference of WNV NS2B/NS3 protease revealed that the natural substrates contain a highly conserved arginine residue in the P₁ position. Further studies showed that basic amino acids were also preferred in P₂ as well as in the P₃ positions^{10,11}.

Until now the most potent inhibitors of NS2B/NS3 protease have been reported by Stoermer et al.¹¹. These compounds are tripeptide aldehydes (**1,2**) with a modified N-capping group (Figure 1). Although inhibitors **1** and **2** displayed low K_i values of 6 and 9 nM, respectively, due to the high reactivity of an aldehyde group, low stability and tendency to form hemiaminals, their application as potential therapeutics is limited¹². Hammamy et al. presented a series of decarboxylated substrate analogues containing chlorophenylacetyl (**3**) or phenylacetyl moiety as an N-capping group which are one of the most potent reversible NS2B/NS3 inhibitors reported thus far¹³. Recently, Bastos et al. presented an interesting group of novel peptide-hybrids reversible inhibitors based on 2,4-thiazolidinedione scaffold (**4**)¹⁴. An interesting reversible inhibitor of NS2B/NS3 was described by Behnam et al.¹⁵ compound **5** containing a benzyloxyphenylglycine residue at P1 position showed a significant reduction of Dengue and WNV titres in cell-based assays of virus replication (EC₅₀ = 15.5 μ M).

Herein, we present the synthesis and application of α -aminoalkylphosphonates and their peptidyl derivatives as NS2B/NS3 WNV protease inhibitors. These compounds belong to a class of irreversible inhibitors that specifically and exclusively react with the active site serine residue leading to the formation of a slow

CONTACT Józef Oleksyszyn  jozef.oleksyszyn@pwr.edu.pl  Faculty of Chemistry, Division of Medicinal Chemistry and Microbiology, Wrocław University of Science and Technology, Wybrzeże Wyspińskiego 27, Wrocław 50-370, Poland

 Supplemental data for this article can be accessed [here](#).

© 2018 The Author(s). Published by Informa UK Limited, trading as Taylor & Francis Group.

This is an Open Access article distributed under the terms of the Creative Commons Attribution License (<http://creativecommons.org/licenses/by/4.0/>), which permits unrestricted use, distribution, and reproduction in any medium, provided the original work is properly cited.

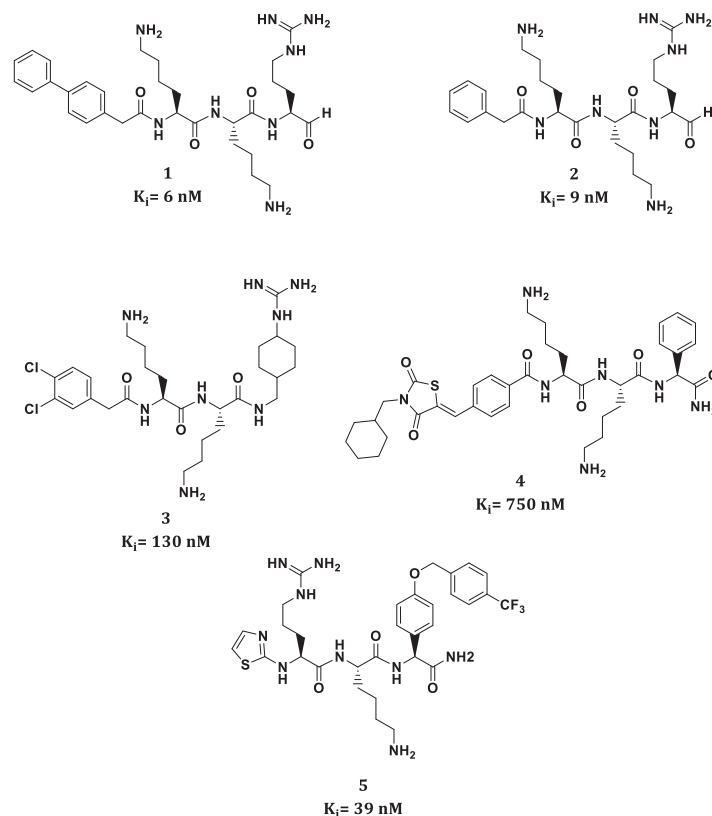
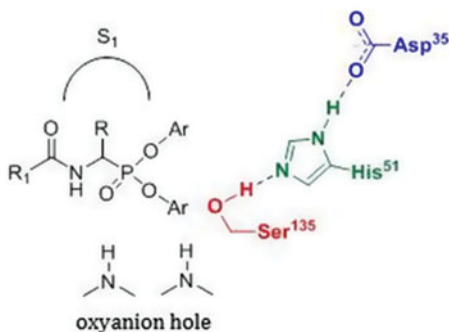
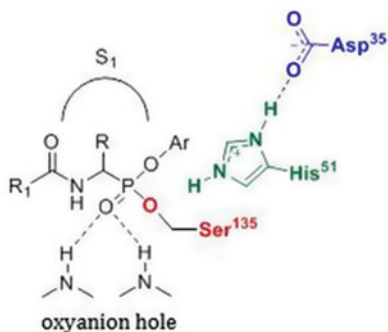


Figure 1. Inhibitors of the West Nile virus NS2B/NS3 protease.

(A) non-covalent complex



(B) non-aged complex



(C) aged complex

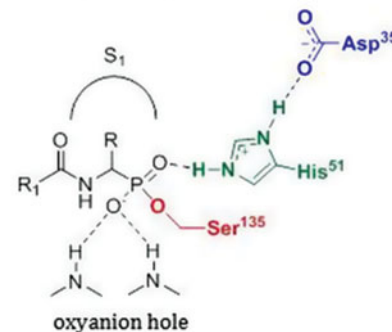


Figure 2. Mechanism of serine proteases inhibition by α -aminoalkylphosphonate diphenyl esters. Residue numbering according to the West Nile virus NS2B/NS3 protease.

hydrolysing protease-inhibitor complex (Figure 2)¹⁶. One of the major advantages of α -aminoalkylphosphonate diphenyl esters is their lack of reactivity with cysteine, aspartyl, and metalloproteases as well as good stability in buffer and human plasma^{17,18}. In this work, we present a series of lysine, arginine, and peptidyl diphenylphosphonate derivatives which could be considered as starting templates for further structure optimisation studies as NS2B/NS3 protease inhibitors.

Chemistry

Chemical reagents

(Benzotriazol-1-yloxy)tripyrrolidinophosphonium hexafluorophosphate (PyBOP), CbzLys(Boc)-OH, Fmoc-Arg(Pbf)-OH, 2-chlorotrityl resin, trifluoroacetic acid, triisopropylsilane (TIPS), N,N-diisopropylethylamine (DIPEA), and di-*tert*-butyl dicarbonate (Boc₂O) were

purchased from IRIS Biotech (Marktredwitz, Germany). All other reagents, catalysts and solvents were purchased either from Sigma-Aldrich (Poznań, Poland), Merck (Warszawa, Poland), or Alfa Aesar (Karlsruhe, Germany).

Inhibitors synthesis

The synthesis of simple Cbz-protected α -aminoalkylphosphonate diphenyl esters (**6–27**) was performed as previously reported^{19,20}. For the overall synthetic strategy as well as the spectroscopic data of the obtained key intermediates and new products, see the [Supplementary material](#) associated with the manuscript. The spectroscopic data for already known compounds fully agreed with the literature data. Briefly, the synthesis of ornithine (**9**) and lysine (**6**) diphenylphosphonates started with the preparation of N-phthalimide-protected amino aldehydes, which were further used

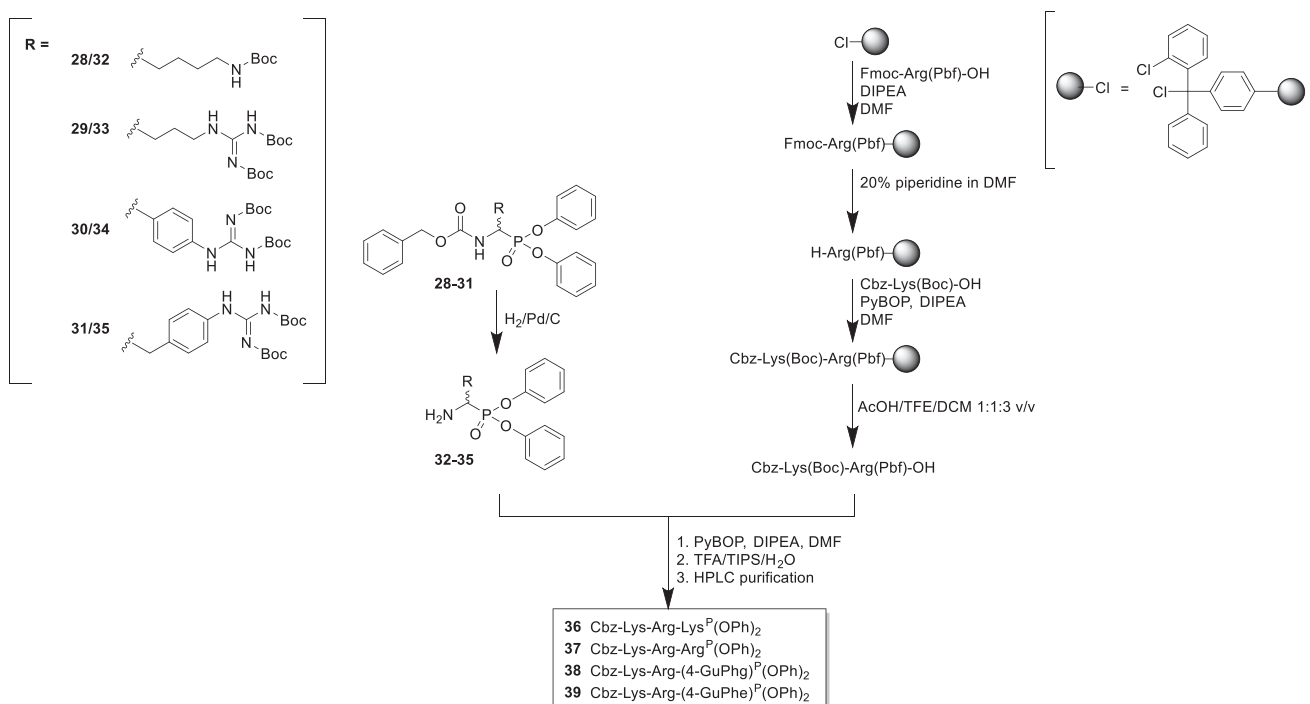


Figure 3. Synthesis of peptidyl α -aminoalkylphosphonate diphenyl esters (**35–38**) of general formula Cbz-Lys-Arg-Aaa^P(OPh)₂, where Aaa^P is a phosphonate ester analogue of arginine.

in the α -amidoalkylation reaction with benzyl carbamate and triphenyl phosphite (Scheme S1.A and S1.B)²⁰. The phthalimide group of resulting orthogonally protected derivatives was removed with hydrazine hydrate, which led to the target compounds²¹. Their subsequent guanidinylation with *N,N*-di-Boc-*S*-ethyl isothiourrea in the presence of HgCl₂ and triethylamine followed by Boc deprotection (50% TFA in DCM) resulted in diphenylphosphonate analogues of arginine (**7**) and homoarginine (**10**)²². In order to synthesise phosphonate analogue of thio-arginine (**8**), 4-chlorobutylaldehyde obtained under Swern conditions from 4-chlorobutane-1-ol was used in the amidoalkylation reaction with benzyl carbamate and triphenyl phosphite with Cu(CF₃SO₃)₂ as a catalyst (Scheme S2)²³. The obtained product was treated with thiourea in refluxing ethanol yielding target compound which crystallised as white solid from diethyl ether. The synthesis of diphenylphosphonate glutamine from 4-oxo-*N*-tritylbutanamide followed the procedure Ewa et al. (Scheme S3)²⁴. The synthesis of 4-amino (**12**) and 4-guanidine (**13**) derivatives of diphenylphosphonate phenylalanine started from the esterification of 4-nitrophenylacetic acid with methanol followed by the reduction of nitro group (Scheme S4). After Boc protection of the amino group, the ester function was reduced to alcohol and then oxidised, by means of the Swern method. Subsequently, α -amidoalkylation with benzyl carbamate and triphenyl phosphite under mild conditions with Cu(CF₃SO₃)₂ as catalyst produced Cbz-(4-*N*-Boc)Phe^P(OPh)₂. Boc deprotection with 50% TFA in DCM gave **12**, which was further transformed into **13** as described above (for derivatives **7** and **10**)²⁵. A similar approach was applied for the synthesis of diphenylphosphonate phenylglycine derivatives (**14–19**) with the exception of nitrobenzaldehyde that was used for phosphonates synthesis, followed by nitro group reduction with SnCl₂ prior to the guanylation step (Scheme S5)²⁶. The synthesis of amidines **21** and **23** from the corresponding nitriles (**20** and **22**) followed the protocol developed by Oleksyszyn et al. (Scheme S6 and S7)^{20,27}. Heterocyclic derivatives of diphenylphosphonate phenylglycine analogue (**24–27**) were obtained *via*

the original α -amidoalkylation reaction procedure with substituted benzaldehydes obtained from 4-fluorobenzaldehyde and appropriate heterocyclic secondary amine (Scheme S8): pyrazole (**24**), benzimidazole (**25**), *N*-methylpiperazine (**26**), or morpholine (**27**)^{20,28}.

For the Cbz-protected derivatives that are most active against NS2B/NS3 protease, we extended their structure with a dipeptidyl Cbz-Lys-Arg fragment. The synthetic strategy, outlined in Figure 3, started with the removal of the Cbz protecting group in orthogonally protected phosphonates *via* hydrogenation over 10% Pd/C, yielding target derivatives (**32–35**) containing a free amino group. In parallel, the Cbz-Lys(Boc)-Arg(Pbf)-OH was synthesised using solid phase peptide synthesis approach on 2-chlorotrityl resin. Next, the obtained phosphonate analogues of arginine were coupled to Cbz-Lys(Boc)-Arg(Pbf)-OH using PyBOP as the coupling agent in the presence of DIPEA. The reaction was performed in DMF for 12 h. The reaction mixture was then diluted five times with ethyl acetate and washed with 5% citric acid, 5% NaHCO₃, and brine. The organic phase was dried over anhydrous MgSO₄, filtered and evaporated to dryness. The obtained crude product was treated with cleavage solution (95% TFA, 2.5% TIPS, 2.5% H₂O; v/v/v) for 2 h at room temperature prior to the precipitation of deprotected phosphonate peptides with diethyl ether. The final compounds were purified on the HPLC (Varian ProStar 210 with a dual λ absorbance detector system equipped with the Discovery[®] BIO Wide Pore C8 HPLC Column 250 mm \times 212 mm, 10 μ m) with a 15 ml/min flow rate using a gradient 5–95% (0.05% TFA/acetonitrile) in (0.05% TFA/H₂O) over 15 min (Method A) or Discovery[®] BIO Wide Pore C8 HPLC Column (250 mm \times 46 mm, 10 μ m) with a 0.9 ml/min flow rate using a gradient 0–100% (0.05% TFA/acetonitrile) in (0.05% TFA/H₂O) over 15 min (Method B)). The nuclear magnetic resonance spectra (¹H and ³¹P) were recorded on either a Bruker Avance DRX-300 (300.13 MHz for ¹H NMR, 121.50 MHz for ³¹P NMR) or Bruker Avance 600 MHz (600.58 MHz for ¹H NMR, 243.10 MHz for ³¹P NMR) spectrometer. Chemical shifts are reported in parts per million (ppm) relative to a tetramethylsilane

internal standard. High-resolution mass spectrometry was acquired on Waters Acquity Ultra Performance LC, LCT Premier, XE.

In vitro NS2B/NS3 protease inhibition

For the initial screening, Cbz-protected aminophosphonates were assayed in 96 well microplates (Nunc™ F96 MicroWell™ White Polystyrene Plate) in the following protease buffer: 50 mM Tris, 1 mM Chaps, 20% glycerol, pH 8.5. WNV NS2B/NS3 protease (AnaSpec, Liege, Belgium; 20 nM) was pre-incubated with tested inhibitor (100 μM) in the protease buffer at 37 °C for 10 min prior an addition of the fluorescent substrate Pyr-RTKR-AMC (AnaSpec, Liege, Belgium; 20 μM). The progress of the reaction was monitored continuously ($\lambda_{\text{ex}} = 354 \text{ nm}$, $\lambda_{\text{em}} = 442 \text{ nm}$) at 37 °C on a Spectra Max Gemini XPS spectrofluorometer (Molecular Devices, Sunnyvale, CA) for 30 min. For compounds which exhibited more than 50% of inhibition, the K_i and k_2/K_i values were calculated. In 96 well microplates narrowed concentration of inhibitors and constant substrate concentration (Pyr-RTKR-AMC, $C = 20 \text{ μM}$, $K_M = 59 \text{ μM}$) were prepared. The enzyme solution was added and enzymatic reaction was monitored (Figure S1). Using a model for irreversible inhibition, in which the first order inactivation rate constant k_{obs} is hyperbolic dependent from the inhibitor concentration K_i and k_2/K_i values were calculated (equations (1–4) in supplementary material)²⁹. Control progress curves in the absence of inhibitor were linear. The standard deviation for the presented values was calculated using the mean of two independent experiments and did not exceed 10%.

Control proteases inhibition assay

Bovine β -trypsin (AppliChem, Łódź, Poland), human cathepsin G (Biocentrum, Kraków, Poland) and Human Airway Trypsin-like Protease (HAT) (R&D Systems, Minneapolis, MN) were used as control proteases to screen the activity of NS2B/NS3 protease inhibitors (**36–39**) obtained in this study. Inhibitors were assayed in 96-well microplates in the 0.1 M HEPES, 0.5 M NaCl, 0.03%, pH 7.5 Triton X-100 (for bovine β -trypsin and cathepsin G). Bovine β -trypsin (15 nM), human cathepsin G (150 nM) or HAT protease (0.001 μg) was pre-incubated with tested inhibitor (25 μM) in the protease buffer at 37 °C for 10 min prior to the addition of the fluorescent substrate: Cbz-Arg-AFC (synthesised in-house according to the procedure described by Bissell³⁰; 50 μM; $\lambda_{\text{ex}} = 400 \text{ nm}$, $\lambda_{\text{em}} = 505 \text{ nm}$, for bovine β -trypsin); MeO-Suc-Ala-Ala-Pro-Val-AMC

(Bachem, Bubendorf, Switzerland; 40 μM, $\lambda_{\text{ex}} = 340 \text{ nm}$, $\lambda_{\text{em}} = 440 \text{ nm}$, for human cathepsin G) or Phe-Ser Arg-AMC (Bachem, Bubendorf, Switzerland; 40 μM, $\lambda_{\text{ex}} = 340 \text{ nm}$, $\lambda_{\text{em}} = 440 \text{ nm}$, for HAT protease). The progress of the reactions was monitored continuously at 37 °C on a Spectra Max Gemini XPS spectrofluorometer for 20 min. Control curves in the absence of inhibitor were linear. The rate of the tested protease inhibition was calculated from the linear range of the plot.

Molecular docking

In order to evaluate the binding mode of the obtained phosphonate inhibitors into the NS2B/NS3 active site, we have performed a molecular docking simulation (AutoDock Vina 1.1.2) using the WNV NS2B/NS3 protease (2fp7.pdb) as a receptor³¹. The coordinates of the Bz-Nle-Lys-Arg-Arg-H inhibitor molecule as well as water molecules were removed from the structure (Figure 4)³². Since numerous studies have shown that α -aminoalkylphosphonates inhibitors complex serine proteases as phosphonic acids, we docked energy minimised (MM2 force field) inhibitor **38** in the chemical form of (Cbz-Lys-Arg-(4-GuPhe)^P(OH)₂)^{33,34}. The centre of the grid box was defined at the catalytic Ser hydroxyl oxygen with the grid box size 100 × 100 × 100 Å. Pictures were prepared in Pymol³⁵.

Results and discussion

Inhibitor P₁ position screening

Compounds presented in this study are categorised into three groups: (I) compounds **6–11** are simple diphenyl phosphonate analogues of lysine, arginine, glutamine, ornithine, homoarginine, and thioarginine; (II) compounds **12–23** are aromatic analogues bearing a basic moiety, and (III) derivatives of diphenylphosphonate phenylglycine (**24–27**) with different heterocyclic substituents. From all tested simple Cbz-N-capped derivatives, the highest potency of action toward NS2B/NS3 protease was observed for compounds **6**, **7**, **13**, and **16** (Table 1). The most potent compound was observed to be **13** with k_2/K_i value of 200 M⁻¹s⁻¹. Replacing the guanidine moiety in **13** with amino group (**12**) resulted in a dramatic drop in the inhibitory activity (11% of inhibition at 100 μM). In general, derivatives substituted at the *meta* position showed weaker inhibition levels as compared to their analogues substituted at *para* position of the phenyl ring (**14**, **15**, **16** vs. **17**, **18**, **19**). Compounds with heterocycles (**24–27**) showed

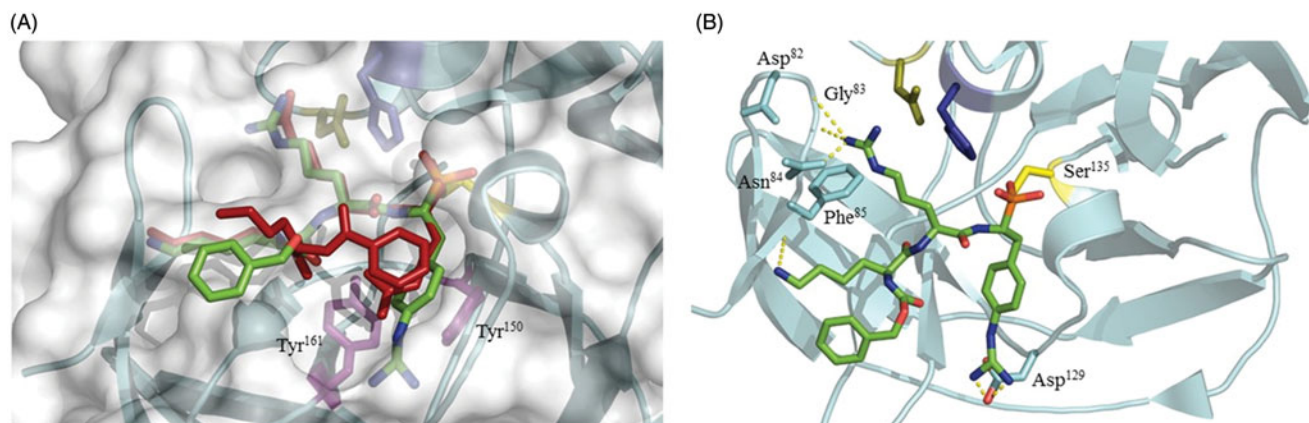


Figure 4. (A) Docking conformation of Cbz-Lys-Arg-(4-GuPhe)^P(OH)₂ (**38**, green) in the binding site of NS2B/NS3 protease. The peptidyl inhibitor is shown in red (Bz-Nle-Lys-Arg-Arg-H) is present in the original crystal structure of WNV protease (2fp7.pdb). (B) Interaction of Cbz-Lys-Arg-(4-GuPhe)^P(OH)₂ (**38**, orange) with the NS2B/NS3 active site. The hydrogen bond network is indicated with yellow dashed lines.

Table 1. Activities of simple Cbz N-capped phosphonates against the NS2B/NS3 WNV protease.^a

No	R	K_i [μM] ^b	k_2/K_i [$\text{M}^{-1}\text{s}^{-1}$]
6		22 ± 2 μM	80
7		13 ± 1 μM	154
8			22%
9			12%
10			12%
11			15%
12			11%
13		4 ± 0.3 μM	200
14			3%
15			16%
16		10 ± 1 μM	87
17			4%
18			8%
19			11%
20			8%
21			22%
22			2%
23			12%
24			5%

(continued)

Table 1. Continued.

No	R	K_i [μM] ^b	k_2/K_i [$\text{M}^{-1}\text{s}^{-1}$]
25			4%
26			3%
27			1%

^aMean values ± standard deviation of two experiments conducted in duplicates.
^bpercent of inhibition was calculated for compounds which displayed low activity toward NS2B/NS3 protease after 30 min incubation at 37 °C; substrate used: Pyr-RTKR-AMC (C = 20 μM , K_M = 59 μM). Bold values indicate the most active compounds.

Table 2. Activities of the peptide phosphonates against the NS2B/NS3 WNV protease^a

No.	Compound	K_i (μM)	k_2/K_i ($\text{M}^{-1}\text{s}^{-1}$)
36	Cbz-Lys-Arg-Lys ^P (OPh) ₂	8 ± 0.9	5 520
37	Cbz-Lys-Arg-Arg ^P (OPh) ₂	3 ± 0.3	10 725
38	Cbz-Lys-Arg-(4-GuPhe) ^P (OPh) ₂	0.4 ± 0.03	28 265
39	Cbz-Lys-Arg-(4-GuPhg) ^P (OPh) ₂	0.7 ± 0.2	24 890
40	Cbz-Lys-Arg-Arg-H	0.12 ± 0.02	Not determined

^aMean values ± standard deviation of two experiments conducted in duplicates. Bold value indicates the most active compound.

very weak (1–5%) inhibition against NS2B/NS3 protease when used at 100 μM concentration. This was probably because the heterocyclic group could not fit into the P1 binding pocket. The phenyl (**21**) and naphthyl (**23**) amidines were slightly more active against the tested protease. Nevertheless, among the tested series of α -aminoalkylphosphonate diphenyl esters we selected the most active compounds for further modifications. In summary, we identified lysine (**6**) and arginine (**7**) as the most favourable P₁ residues, whereas for non-proteinogenic amino acid analogues we selected guanidine derivatives (**13**) and p (**16**)²³.

Influence of peptide chain elongation

The structure of the most active inhibitors identified in the initial screening step was elongated with a P₂ Arg and P₃ Lys. The resultant compounds (**36–39**) showed significantly increased inhibitory potencies against NS2B/NS3 protease (Table 2). The introduction of the additional two residues into the structure resulted in a similar (69-fold) improvement in their inhibitory potency, leading to **36** (k_2/K_i = 5 520 $\text{M}^{-1}\text{s}^{-1}$) and **37** (k_2/K_i = 10 725 $\text{M}^{-1}\text{s}^{-1}$). The most potent NS2B/NS3 protease inhibitor identified in the presented studies was compound **38**, which displayed a k_2/K_i value of 28 265 $\text{M}^{-1}\text{s}^{-1}$. The highest (~290-fold) increase of inhibitory potencies was observed for the peptidyl derivative of the phosphonate analogue of 4-guanidinephenylglycine (**39**) which showed a k_2/K_i value of 24 890 $\text{M}^{-1}\text{s}^{-1}$. The inhibition data observed for **36–39** is in agreement with the reported X-ray structure of NS2B/NS3 protease, thus highlighting the significant role of P₂ and P₃ residues in binding molecules (substrates and inhibitors) to the enzyme³². As reference compound we synthesised peptide aldehyde inhibitor (**40**). This reversible inhibitor

showed K_i lower (~4 times) than our most potent phosphonate inhibitor. However, it is difficult to compare the K_i values between reversible and irreversible inhibitors. Noteworthy, all of the obtained compounds were tested as diastereoisomeric mixtures thus their separation into single isomers will lead to significantly more potent inhibitors as observed previously³⁶. Further investigation into the design and synthesis of phosphonate inhibitors of NS2B/NS3 protease might lead to discovering more potent and selective inhibitors. Future work should involve structure-activity relationship studies of the P2 and P3 residues as well as ring substituents. The next challenge is a more comprehensive structure-activity relationship study aiming to optimise the peptidyl fragment of the inhibitor as well as the structure of the aromatic ring substituent prior to the *in vivo* studies of most potent derivatives.

Protease selectivity assay

The selectivity of inhibitors **36–39** were determined by means of serine proteases of a similar substrate recognition pattern such as bovine β -trypsin, human cathepsin G, and HAT protease. The results clearly showed that the inhibition levels observed for all of the investigated compounds at a concentration of 25 μ M did not exceed 10% after a 30 min incubation period (Table S2). These results indicate that the obtained peptidyl inhibitors are not significantly active against members of proteases with a trypsin-like activity. However, the selectivity toward other members of this family will be further examined.

Molecular docking

The analysis of inhibitor **38** docked to the active site of NS2B/NS3 protease revealed docking conformation to be very similar to the one observed for Bz-Nle-Lys-Arg-Arg-H present in the crystal structure reported by Erbel et al. (2fp7.pdb)³². The reactive phosphonate warhead of the inhibitor is in close proximity (1.6 Å) to the catalytic serine residue allowing the formation of a covalent bond between the protease and inhibitor (Figure 4(A), Figure S3). The basic side chains of the amino acids in P₁ and P₃ positions are responsible for the formation of an extensive hydrogen bonding network with the protease (Figure 4(B)) including the P₁ 4-guanidinophenylalanine electrostatic interaction with the side chain of Asp129; P₂ arginine with the carbonyl oxygen of Gly83, and Asp82 and the side chain of Asn84; and lysine in P₃ position with Phe85 carbonyl oxygen. Additionally, two tyrosine residues (Tyr150, Tyr161) could be responsible for interaction with aromatic ring of 4-guanidinophenylalanine inhibitor residue (Figure 4(A), Figure S4). This interaction provides explanation for the improved activity of inhibitors **38** and **39** over simple lysine and arginine analogues (**36,37**).

Conclusions

In this work, we present a series of phosphonate diphenyl esters with low micromolar inhibitory activities against the WNV NS2B/NS3 protease. This class of inhibitors has never been reported to inhibit the NS2B/NS3 protease. The rigid 4-guanidinophenylalanine and 4-guanidinophenylglycine moieties at the P1 position were found to be more potent than a P1 arginine. Future work should involve more structure-activity relationship studies at the P2 and P3 residues and changing the phosphonate ester moieties.

Acknowledgements

The authors would like to thank Dr. Ewa Burchacka and Maciej Walczak for the kind gift of Cbz-Gln^P(OPh)₂ and Dr. Renata Grzywa for guidance in the inhibitors docking analysis.

Disclosure statement

No potential conflict of interest was reported by the authors.

Funding

This work was supported by the Ministry of Science and Higher Education's Iuventus Plus Programme [IP2012 0556 72]. The funder had no role in the study design, data collection and analysis, decision to publish, or preparation of the manuscript. MS and JO are grateful to Wroclaw University of Technology for support [Statute Funds 0401/0195/17]. MS is grateful to National Science Centre [UMO-2013/09/N/ST5/02439]. AM and KP are grateful to National Science Centre [UMO-2016/21/B/NZ6/01307]. Project supported by Wroclaw Centre of Biotechnology, programme The Leading National Research Centre (KNOW) for years 2014–2018.

References

1. Smithburn KC, Hughes TP, Burke AW, Paul JH. A neurotropic virus isolated from the blood of a native of Uganda. *Am J Trop Med Hyg* 1940;1:471–92.
2. Lanciotti RS, Roehrig JT, Deubel V, et al. Origin of the West Nile virus responsible for an outbreak of encephalitis in the northeastern United States. *Science* 1999;286:2333–7.
3. McMullen AR, May FJ, Li L, et al. Evolution of new genotype of West Nile virus in North America. *Emerging Infect Dis* 2011;17:785–93.
4. Centers for Disease Control and Prevention CDC [cited 2018 Sept 5]. Available from: www.cdc.gov/westnile/index.html
5. Sejvar JJ. West Nile virus: an historical overview. *Ochsner J* 2003;5:6–10.
6. Colpitts TM, Conway MJ, Montgomery RR, Fikrig E. West Nile virus: biology, transmission, and human infection. *Clin Microbiol Rev* 2012;25:635–48.
7. Holbrook MR. Historical perspectives on flavivirus research. *Viruses* 2017;9:97.
8. Suthar MS, Diamond MS, Gale M. West Nile virus infection and immunity. *Nat Rev Microbiol* 2013;11:115–28.
9. Schechter I, Berger A. On the size of the active site in proteases. I. Papain. *Biochem Biophys Res Commun* 1967;27:157–62.
10. Chappell KJ, Stoermer MJ, Fairlie DP, Young PR. West Nile virus NS2B/NS3 protease as an antiviral target. *Curr Med Chem* 2008;15:2771–84.
11. Stoermer MJ, Chappell KJ, Liebscher S, et al. Potent cationic inhibitors of West Nile virus NS2B/NS3 protease with serum stability, cell permeability and antiviral activity. *J Med Chem* 2008;51:5714–21.
12. Kisselev AF, Goldberg AL. Proteasome inhibitors: from research tools to drug candidates. *Chem Biol* 2001;8:739–58.
13. Hammamy MZ, Haase C, Hammami M, et al. Development and characterization of new peptidomimetic inhibitors of the West Nile virus NS2B-NS3 protease. *ChemMedChem* 2013;8:231–41.

14. Bastos LA, Behnam MA, El Sherif Y, et al. Dual inhibitors of the dengue and West Nile virus NS2B-NS3 proteases: synthesis, biological evaluation and docking studies of novel peptide-hybrids. *Bioorg Med Chem* 2015;23:5748–55.
15. Behnam MAM, Graf D, Bartenschlager R, et al. Discovery of nanomolar dengue and West Nile virus protease inhibitors containing a 4-benzyloxyphenylglycine residue. *J Med Chem* 2015;58:9354–70.
16. Oleksyszyn J, Powers JC. Irreversible inhibition of serine proteases by peptidyl derivatives of alpha-aminoalkylphosphonate diphenyl esters. *Biochem Bioph Res Co* 1989;161:143–9.
17. Oleksyszyn J, Powers JC. Irreversible inhibition of serine proteases by peptide derivatives of (alpha-aminoalkyl)phosphonate diphenyl esters. *Biochemistry* 1991;30:485–93.
18. Sienczyk M, Oleksyszyn J. Irreversible inhibition of serine proteases – design and *in vivo* activity of diaryl alpha-amino-phosphonate derivatives. *Curr Med Chem* 2009;16:1673–87.
19. Oleksyszyn J, Powers JC. Amino acid and peptide phosphonate derivatives as specific inhibitors of serine peptidases. *Methods in Enzymology* 1994;244:423–441.
20. Oleksyszyn J, Subotkowska L, Mastalerz P. Diphenyl 1-amino-alkanephosphonates. *Synthesis* 1979;1979:985–6.
21. Hamilton R, Walker BJ, Walker B. A convenient synthesis of N-protected diphenyl phosphonate ester analogues of ornithine, lysine and homolysine. *Tetrahedron Lett* 1993;34:2847–50.
22. Peterlin-Mašič L, Kikelj D. Arginine mimetics. *Tetrahedron* 2001;57:7073–105.
23. Van der Veken P, El Sayed I, Joossens J, et al. Lewis acid catalyzed synthesis of N-protected diphenyl 1-aminoalkyl-phosphonates. *Synthesis* 2004;2005:634–8.
24. Ewa B, Maciej W, Marcin S, et al. The development of first *Staphylococcus aureus* SplB protease inhibitors: phosphonic analogues of glutamine. *Bioorg Med Chem Lett* 2012;22:5574–8.
25. Joossens J, Van der Veken P, Lambeir AM, et al. Development of irreversible diphenyl phosphonate inhibitors for urokinase plasminogen activator. *J Med Chem* 2004;47:2411–3.
26. Sienczyk M, Oleksyszyn J. A convenient synthesis of new alpha-aminoalkylphosphonates, aromatic analogues of arginine as inhibitors of trypsin-like enzymes. *Tetrahedron Lett* 2004;45:7251–4.
27. Oleksyszyn J, Boduszek B, Kam CM, Powers JC. Novel amidine-containing peptidyl phosphonates as irreversible inhibitors for blood coagulation and related serine proteases. *J Med Chem* 1994;37:226–31.
28. Magdolen P, Meciariova M, Toma S. Ultrasound effect on the synthesis of 4-alkyl-(aryl)aminobenzaldehydes. *Tetrahedron* 2001;57:4781–5.
29. Stein RL, Trainor DA. Mechanism of inactivation of human leukocyte elastase by a chloromethyl ketone: kinetic and solvent isotope effect studies. *Biochemistry* 1986;25:5414–9.
30. Bissell ER, Mitchell AR, Smith RE. Synthesis and chemistry of “7-amino-4-(trifluoromethyl)coumarin and its amino-acid and peptide derivatives. *J Org Chem* 1980;45:2283–7.
31. Trott O, Olson AJ. Software news and update autodock vina: improving the speed and accuracy of docking with a new scoring function, efficient optimization, and multithreading. *J Comput Chem* 2009;31:455–61.
32. Erbel P, Schiering N, D’Arcy A, et al. Structural basis for the activation of flaviviral NS3 proteases from dengue and West Nile virus. *Nat Struct Mol Biol* 2006;13:372–3.
33. Hof P, Mayr I, Huber R, et al. The 1.8 angstrom crystal structure of human cathepsin G in complex with Suc-Val-Pro-Phe(P)-(OPh)(2): a janus-faced proteinase with two opposite specificities. *Embo J* 1996;15:5481–91.
34. Lechtenberg BC, Kasperkiewicz P, Robinson H, et al. The elastase-PK101 structure: mechanism of an ultrasensitive activity-based probe revealed. *ACS Chem Biol* 2015;10:945–51.
35. DeLano WL. The PyMOL molecular graphics system. San Carlos (CA): DeLano Scientific; 2002.
36. Winiarski L, Oleksyszyn J, Sienczyk M. Human neutrophil elastase phosphonic inhibitors with improved potency of action. *J Med Chem* 2012;55:6541–53.